Climate Dynamics (2019) 52:5173–5187
https://doi.org/10.1007/s00382-018-4443-5

Preferred solar signal and its transfer in the Asian–Pacific subtropical jet region

Delin Li[1,2] · Ziniu Xiao[1] · Liang Zhao[1]

Received: 17 February 2018 / Accepted: 9 September 2018 / Published online: 12 October 2018

Abstract

Solar impact on the tropospheric subtropical jet (SJ) has been identified previously from a zonally averaged perspective. The SJ was observed to be weaker in the high solar activity winters. However, some regional features of solar-induced SJ variations might remain unrecognized. Here it is found that the regional solar signal in wintertime Asian–Pacific zonal wind at 200 hPa, which exhibits a tripolar banded structure, greatly resembles the second internal mode of zonal wind within the same sector. Significant response of the Asian–Pacific SJ (APSJ) to increased solar forcing in boreal winter exclusively marks its center region, showing a deceleration in westerlies. Further exploration suggests two possible top–down routes to interpret this particular manifestation of solar signal in APSJ center, a tropical route and a middle–high latitude route. Regarding the tropical route, during the cold season, driven by the solar-associated reduction in Brewer–Dobson circulation, ozone concentration in tropical lower stratosphere increases notably and merely within the zonal range of APSJ center. This heats the air here and the tropical tropospheric regional upwelling is thereby suppressed. Consequently, a significant weakened APSJ center is produced via local Hadley cell. Regarding the middle–high latitude route, in early winter, solar-related pronounced westerly anomalies in the mid-latitude stratosphere only appear in the longitudinal range of APSJ center. Meanwhile, the upward propagating planetary waves from the troposphere could be reflected back downward by this intensified stratospheric westerlies. As winter progresses, through wave mean flow interactions, a resultant weakened APSJ center markedly presents in the middle of winter.

Keywords Regional solar signal · Asian–Pacific subtropical jet · Top–down transfer of solar signal · Solar effects

1 Introduction

It is believed that the tiny variations in solar radiation over the 11-year sunspot cycle could affect the large-scale atmospheric circulation. In recent decades, a large body of observational and modeled evidence has accumulated in support of solar impact and modulation of the spatiotemporal variabilities of crucial internal atmospheric modes in the troposphere, including the Arctic Oscillation/North Atlantic Oscillation (AO/NAO) (Kodera 2002, 2003; Kodera and Kuroda 2005; Matthes et al. 2006; Ineson et al. 2011; Gray et al. 2013; Scaife et al. 2013), Northern and Southern Annular Modes (Weng 2012; Kodera et al. 2016; Kuroda and Kodera 2005; Kuroda and Shibata 2006; Roscoe and Haigh 2007; Kuroda and Yamazaki 2010), Pacific/North American pattern (PNA) (Liu et al. 2014; Huth et al. 2006; Li and Xiao 2018), among others. Meanwhile, close connections between these internal atmospheric modes and the tropospheric subtropical jet (SJ) have been identified (e.g. Ambaum et al. 2001; Li and Wang 2003; Codron 2007; Hinssen et al. 2010). For instance, Ambaum et al. (2001) demonstrated that the PNA was related to the variability in the SJ exit over the North Pacific region, and also showed a strong association between the NAO and the North Atlantic SJ. Therefore, there is the possibility that the variability in regional tropospheric SJ could also be partly influenced by the small changes in solar activity.

✉ Ziniu Xiao
xiaozn@lasg.iap.ac.cn

Delin Li
ldl@lasg.iap.ac.cn

1 State Key Laboratory of Numerical Modeling for Atmospheric Sciences and Geophysical Fluid Dynamics, Institute of Atmospheric Physics, Chinese Academy of Sciences, Beijing, China

2 University of Chinese Academy of Sciences, Beijing, China

Previous studies have already revealed the relationship between solar activity and the tropospheric SJ in both the North and South Hemispheres. In observational data analyses, it has been noted that the SJ decelerates and shifts poleward under solar maxima compared to solar minima (Crooks and Gray 2005; Misios and Schmidt 2013), together with a poleward expansion of Hadley cell (Gleisner and Thejll 2003; Kodera et al. 2016). Using numerical models, some works have reported that the tropospheric atmosphere response to increased solar forcing appears as a weakened SJ with slight poleward displacement, accompanied by a weakened and broadened Hadley cell (Haigh 1996; Shindell et al. 1999; Haigh et al. 2005; Haigh and Blackburn 2006; Rind et al. 2008; Meehl et al. 2009). While others have suggested that the Hadley circulation becomes stronger in solar maxima than in solar minima (van Loon et al. 2004, 2007). However, most studies have only considered the global zonal mean zonal wind when investigating the association between tropospheric SJ and solar activity, and some regional solar signals in the tropospheric SJ might remain unrecognized.

The upper-tropospheric SJ, whose strongest center locates over East Asia and the western North Pacific, is an important atmospheric circulation system linked closely to the weather and climate across the Asian–Pacific region. The Asian–Pacific SJ (APSJ) is not only characterized by notable seasonal fluctuations, but also has pronounced variation in its strength and position on interannual timescales (Liang and Wang 1998; Kuang and Zhang 2005; Lin and Lu 2005; Xie et al. 2015; Hong and Lu 2016). Although the APSJ is relatively stable during boreal winter, its associations with interannual wintertime climate changes in its upstream and downstream regions have been demonstrated by several studies. For example, intensified East Asian SJ was connected to strengthened East Asian winter monsoon, East Asian trough, Aleutian low, and western North American ridge, resulting in colder winters over East Asia and warmer winters over the western United States (Yang et al. 2002; Jhun and Lee 2004).

Some factors, such as the El Niño/Southern Oscillation (ENSO) and stratospheric dynamic and thermal conditions, can affect the variations in tropospheric SJ. ENSO is usually regarded as a strong forcing for the year-to-year variability of extratropical atmosphere, especially over the Asian–Pacific sector. The tropical sea surface temperature (SST) anomalies of ENSO events exert great influence on SJ through the changes in Hadley cell intensity (Arkin 1982; Oort and Yienger 1996; Seager et al. 2003). The APSJ strengthens (weakens) the most to the east of the dateline over the North Pacific during the warm (cold) ENSO years (Chen and van den Dool 1999; Quadrelli and Wallace 2002; Yang et al. 2002; Seager et al. 2005; Andreoli and Kayano 2005). At the same time, the dynamic and thermal changes in stratosphere can actually alter the strength and latitude of tropospheric westerlies via the coupling between stratosphere and troposphere. In respect of the effect of stratospheric circulation perturbation on the troposphere, Baldwin and Dunkerton (1999) showed that the large-amplitude anomalies in AO in the stratosphere tended to precede the substantial variation in the tropospheric jet strength. When the stratospheric circumpolar jet was stronger, the upward-propagating planetary waves in the troposphere were mainly refracted toward the equator, and the associated poleward wave momentum fluxes helped maintain the poleward shift of the tropospheric westerlies (Limpasuvan and Hartmann 2000). The tropospheric response to stratospheric variability could also be produced by anomalous stratospheric heating. For instance, stratospheric polar cooling in winter could lead the tropospheric jet to shift poleward through transient eddy mean-flow interactions (Kushner and Polvani 2004). The results from the experiments carried out by Simpson et al. (2009) showed that increased heating in the tropical lower stratosphere could cause northward displacement and weakening of tropospheric jet. They also emphasized the importance of changing eddy momentum fluxes in the tropospheric response to such applied stratospheric heating perturbation. While in response to the high-latitude or latitudinally uniform heating in the lower stratosphere, the tropospheric jet moved equatorward (Haigh et al. 2005).

With these mentioned above in mind, the present study is focusing on the regional solar influence on the wintertime APSJ and the possible mechanism. Section 2 describes the data used in the analysis. In Sect. 3, we investigate the relationship between solar activity and the leading internal modes of upper-tropospheric zonal wind over the Asian–Pacific sector, as well as the characteristics in the response of APSJ to solar forcing. The possible top–down mechanism of solar effects on the tropospheric atmosphere has been noted before (e.g. Kodera and Kuroda 2002; Matthes et al. 2006; Kodera et al. 2016). However, these previous studies were mostly conducted from a zonally averaged perspective. Therefore, in spite of previous efforts, there may be still a lack in revealing the propagating processes of solar signal from the stratosphere to the regional troposphere. Thus, Sect. 4 explores the feasible top–down mechanism of solar influence on the APSJ and presents an explanation of the solar preference for the APSJ. We end with brief conclusion and discussion in Sect. 5.

2 Data

Considering that the intensity of tropospheric APSJ peaks during boreal winter, we averaged climate data for December of the previous year through February of the current year (DJF) and removed their linear trends before the analysis. In this study, the wintertime APSJ center intensity index was defined as DJF-mean 200 hPa zonal wind averaged over its maximum region (above 70 m s^{-1}) of 30°N–36°N, 125°E–160°E (indicated by the red box in Fig. 1c). Similar in most studies, the sunspot number (SSN), which varies with the quasi-11-year cycle, was used as solar activity proxy data. Monthly SSN data were obtained from the World Data Center SILSO of Royal Observatory of Belgium (available at http://sidc.oma.be/silso/) and calculated into DJF means. To investigate the relationship between solar activity and APSJ variability, we used the 200 hPa zonal wind during 1979–2015 with 1°×1° resolution from the ERA-Interim dataset of European Centre for Medium-Range Weather Forecast (ECMWF) (Dee et al. 2011). To test the consistency of solar signal in the APSJ, we used monthly 200 hPa zonal wind data from two reanalysis datasets with different time spans: National Centers for Environmental Prediction/National Center for Atmospheric Research (NCEP/NCAR) data for 1948–2015 with 2.5°×2.5° resolution (Kalnay et al. 1996) and ERA-20C (ECMWF twentieth-century) data for 1900–2010 with 1°×1° resolution (Poli et al. 2013).

Due to a lack of satellite data, there may be some uncertainties in the data of the upper stratosphere before 1979. Therefore, to further explore the propagation of the solar signal from the stratosphere to the tropospheric APSJ, we chose the limited observations available from 1979 onward. The monthly reanalysis data of the U and V components of wind, vertical velocity, temperature, and ozone mass mixing ratio with 1°×1° resolution for 1979–2015 were taken from the ERA-Interim. We adopted outgoing longwave radiation (OLR) as an indicator for atmospheric convection strength. Monthly OLR data at 1°×1° resolution from 1979 to 2012 were provided by the National Oceanic and Atmospheric Administration (NOAA) (Lee 2014). We used the DJF-mean Nino 3.4 index (mean SSTs over 5°S–5°N latitudes and 170°W–120°W longitudes) for 1979–2015 from the NOAA Climate Prediction Center to represent the ENSO variability.

3 Relationship between solar activity and wintertime APSJ variability

To examine the relationship between solar activity and internal variability of the upper-tropospheric APSJ during boreal winter, we extract the leading modes of variability for the DJF-mean 200 hPa zonal wind within the Asian–Pacific region (5°N–70°N, 60°E–120°W) using an empirical orthogonal function (EOF) analysis. Figure 1 shows the first and second EOF modes (EOF1 and EOF2) and the corresponding principal components (PC1 and PC2). The EOF1 explains 44.8% of the total variance, 30.7% more than the EOF2 (14.1%). As displayed in

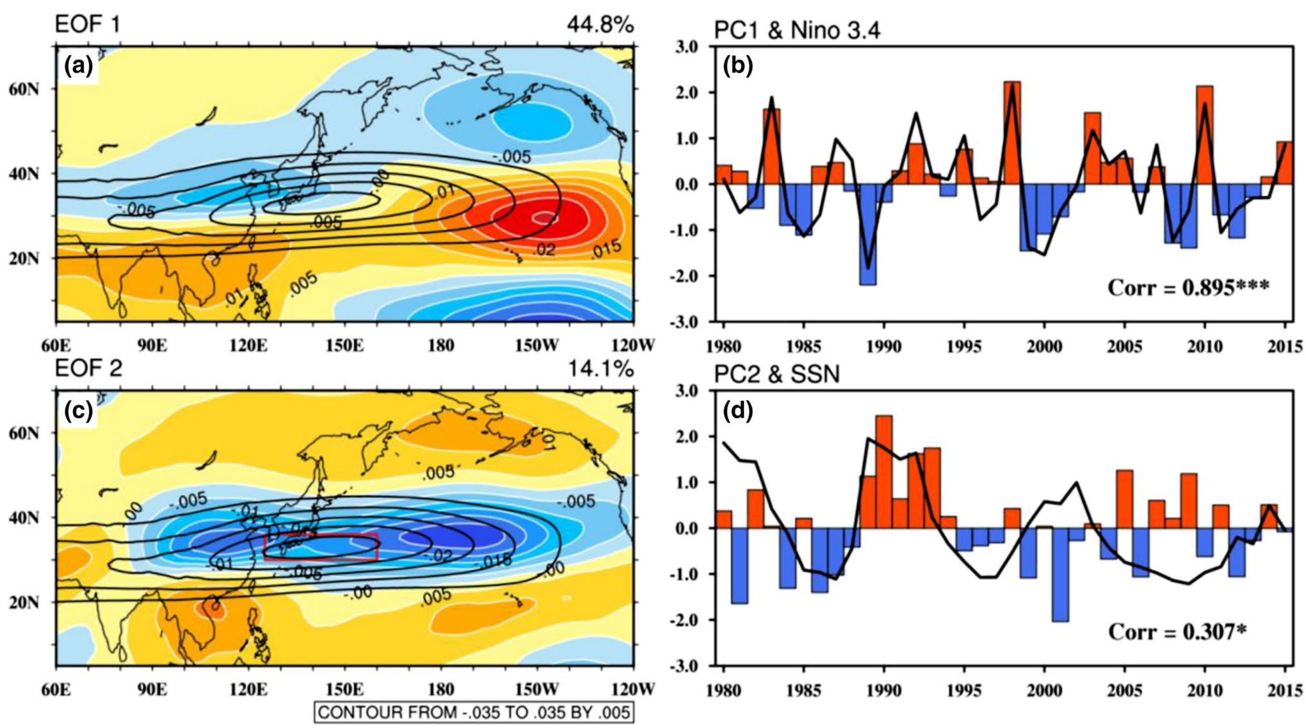

Fig. 1 Spatial patterns of the **a** EOF1 and **c** EOF2 of DJF 200 hPa zonal wind over the Asian–Pacific region for 1980–2015. Black contours in **a** and **c** represent the average zonal wind speed exceeding 30 m s^{-1} and the contour interval is 10 m s^{-1}. The corresponding **b** PC1 and **d** PC2. The superimposed lines in **b** and **d** separately represent the standardized time series of DJF Nino 3.4 index and SSN. Single (triple) asterisk denotes 90% (99%) confidence level for the correlation coefficient. The red box in **c** indicates the APSJ center

Fig. 1a, the EOF1 presents a meridional tripolar structure spanning the central-eastern North Pacific, with two negative regions over the tropics and middle–high latitudes and a positive subtropical region, accompanying a weak north–south dipole pattern in East Asia. In the spatial distribution of EOF1, anomalous westerlies increase the most in the APSJ exit. Thus, the EOF1 mainly features an east–west shift of APSJ. The PC1 is characterized by marked interannual fluctuations (Fig. 1b) and ties closely to the Nino 3.4 index, with a correlation coefficient of 0.895 beyond the 99% confidence level. There is no obvious correlation between PC1 and SSN (correlation coefficient = − 0.100). The EOF2 captures a banded structure spanning the entire Asian–Pacific sector, with easterly anomalies at 20°N–45°N and westerly anomalies on the poleward and equatorward sides (Fig. 1c). Reduced westerlies mainly appear in the APSJ main body in the spatial distribution of EOF2. In addition, the correlation between PC2 and the wintertime APSJ center intensity index is − 0.829, with a 99% confidence level. Therefore, the EOF2 could depict the variability of APSJ center strength. Apart from the interannual variability, a clear interdecadal feature can be seen in PC2 (Fig. 1d). Notably, a significant positive correlation (0.307) is found between PC2 and SSN, with the 90% confidence level. While the relationship between PC2 and the Nino 3.4 index is insignificant (correlation coefficient = 0.152).

The regressions for the DJF-mean 200 hPa zonal wind against the standardized Nino 3.4 index and SSN are presented in Fig. 2a, b. The intensification of Nino 3.4 index is accompanied by a considerable strengthening (> 7 m s^{-1}) of westerlies in the APSJ exit region and a relatively weakened APSJ center (Fig. 2a). The ENSO-regressed pattern is quite similar to the EOF1, with a high spatial pattern correlation of 0.983, indicating that ENSO may be the main influencing factor for EOF1. The robust linkage between ENSO and the dominant mode of Asian–Pacific 200 hPa zonal wind has been well documented in previous studies (e.g. Yang et al. 2002; Ren et al. 2008). Thus, the leading internal mode, which indicates the east–west displacement of the APSJ center, is primarily forced by ENSO. Apparently, the 200 hPa zonal wind anomalies induced by solar activity (Fig. 2b) are distinguished from those caused by ENSO (Fig. 2a). The distribution of regressions in Fig. 2b shows a sandwich pattern spanning East Asia and the North Pacific. The most striking feature in the SSN-regressed pattern is the pronounced deceleration, by about − 1.5 m s^{-1}, in subtropical westerlies over only the APSJ center from 140°E to 150°E with 95% confidence level and from 130°E to 175°E with 90% confidence level. It seems that the APSJ center is an exclusive region preferred by solar activity over

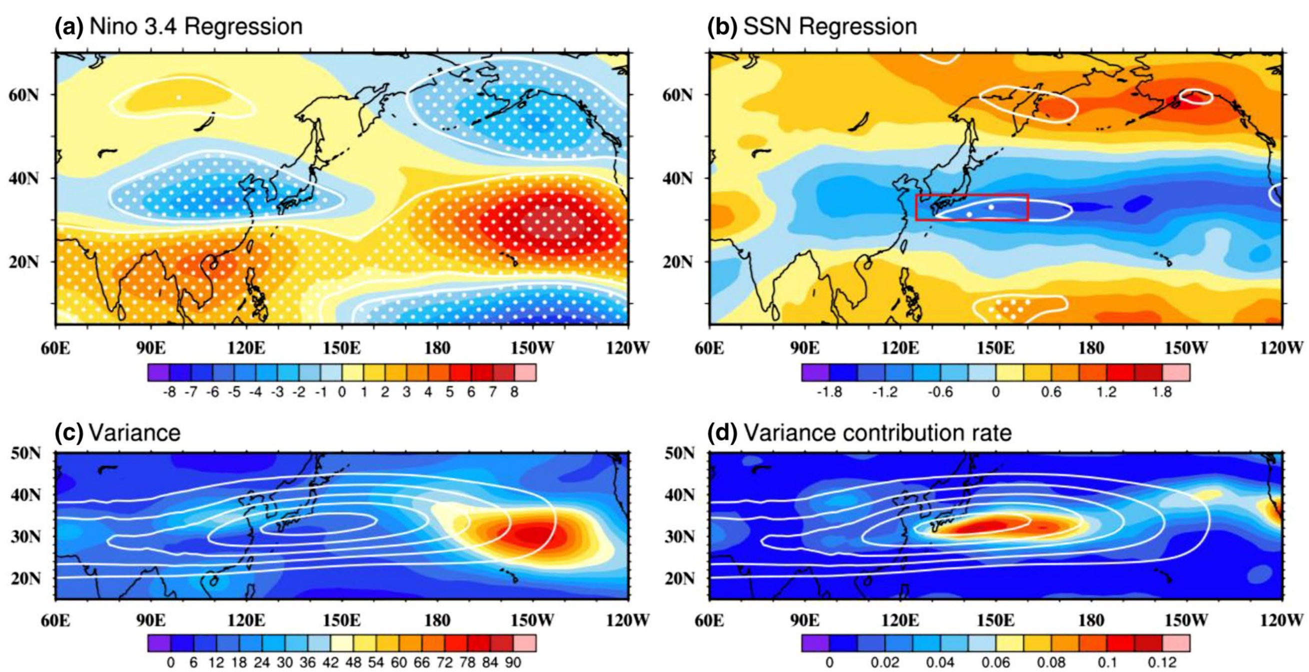

Fig. 2 Regression coefficients between DJF 200 hPa zonal wind and the standardized DJF **a** Nino 3.4 index and **b** SSN. Regression coefficients in **a** and **b** above the 95% (90%) confidence level are highlighted by white dots (white contours). The red box in **b** indicates the APSJ center. **c** Variance (m^2 s^{-2}) of DJF zonal wind at 200 hPa in the APSJ region for 1980–2015. **d** Variance contribution rate (%) of solar-regressed DJF 200 hPa zonal wind anomalies in the APSJ region. White contours in **c** and **d** denote the average zonal wind speed exceeding 30 m s^{-1} and the contour interval is 10 m s^{-1}

the subtropical Asian–Pacific region. It is also intriguing to see that this anomalous tripolar pattern in Fig. 2b bears much resemblance with the EOF2 in Fig. 1c. Meanwhile, the spatial pattern correlation between this SSN-regressed pattern and EOF2 is 0.807, implying that the solar-induced pattern could capture the main signature in the second internal mode of wintertime 200 hPa zonal wind over the Asian–Pacific region. Therefore, this tripolar EOF2 mode, which represents the variability in the APSJ center intensity, might be partly attributed to solar forcing. Besides, the variance of DJF-mean zonal wind at 200 hPa and the variance contribution rate of solar-regressed DJF-mean 200 hPa zonal wind anomalies in the APSJ region for 1980–2015 are respectively given in Fig. 2c, d. The maximal variance ($> 80\ \mathrm{m}^2\ \mathrm{s}^{-2}$) of the 200 hPa zonal wind in winter presents in the exit region of APSJ. It is worth noting that the maximal variance contribution rate ($> 10\%$) of solar-induced 200 hPa zonal wind anomalies finely lies in the APSJ center region. While, the variance contribution rate in other area over the same latitude band of APSJ region is quite small. This further verifies the solar preference for the zonal wind in the APSJ center.

To assess the robustness of the above results based on the ERA-Interim dataset for 1980–2015, we perform EOF and linear correlation analyses for the two other reanalysis datasets with longer time periods: NCEP/NCAR for 1949–2015 and ERA-20C for 1901–2010. As plotted in Fig. 3, the second EOF patterns of DJF-mean 200 hPa zonal wind variability within the Asian–Pacific sector from both datasets are quite similar to that from ERA-Interim, and the confidence levels of the correlations between the PC2s and SSN (95% for NCEP/NCAR and 99% for ERA-20C) are stronger than that of ERA-Interim (90%). As exhibited in Fig. 4, changes in the APSJ center intensity indices calculated from these three datasets show high consistency with those in the corresponding PC2s ($\times -1.0$). Also, we display the associations of SSN with these APSJ center intensity indices (Fig. 4). Although the spans of each time series of APSJ center intensity indices are different, all three correlation coefficients between the APSJ center intensity indices and SSN are marked with high confidence levels (90% for ERA-Interim and ERA-20C, 95% for NCEP/NCAR). Therefore, the overall results from NCEP/NCAR and ERA-20C datasets are in agreement with those from ERA-Interim, further supporting the suggestion that the particular regional solar signal in the Asian–Pacific sector could be interpreted as a weakened APSJ center.

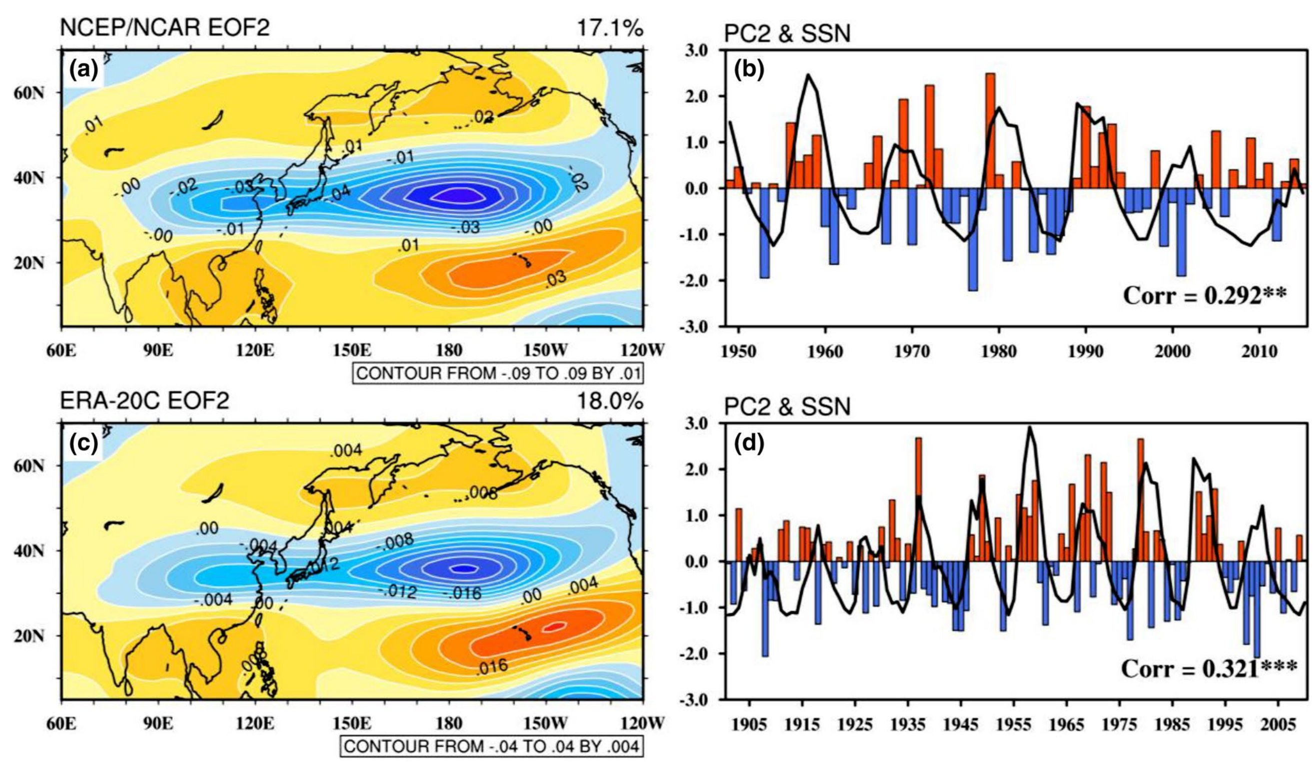

Fig. 3 As in Fig. 1c, d, but for the 200 hPa zonal wind in the NCEP/NCAR dataset for 1949–2015 and the ERA-20C dataset for 1901–2010, respectively. Double (triple) asterisks denote 95% (99%) confidence level for the correlation coefficient

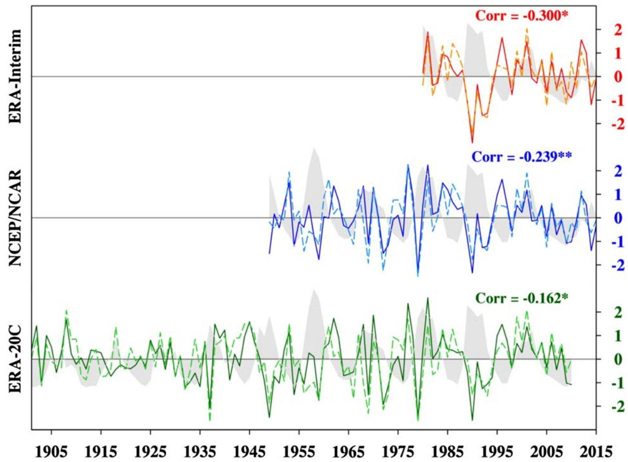

Fig. 4 Standardized time series of DJF APSJ center intensity indices (solid lines) and the PC2s (× − 1.0) (dashed lines) of the wintertime Asian–Pacific 200 hPa zonal wind calculated from the datasets of ERA-Interim (1980–2015), NCEP/NCAR (1949–2015), and ERA-20C (1901–2010). The filled grey lines represent the standardized time series of DJF SSN. Single (double) asterisk denotes the 90% (95%) confidence level for the correlation coefficient between SSN and the APSJ center intensity index

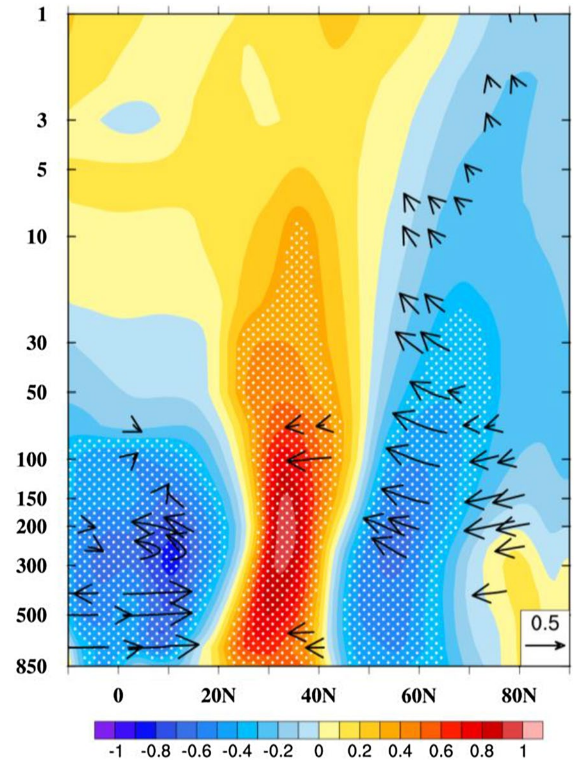

Fig. 5 Correlations of DJF zonal mean (105°E–180°E) zonal wind (color shading) and meridional circulation (arrows) with DJF APSJ center intensity index based on the ERA-Interim dataset. The white dots indicate significant zonal wind above the 95% confidence level. Only meridional circulation above the 95% confidence levels is shown

4 Possible mechanism of solar signal transfer in the Asian–Pacific sector

As revealed above, during boreal winter, the relationship between SSN and the second EOF mode of Asian–Pacific 200 hPa zonal wind or the APSJ center intensity is robust. Over the subtropical Asian–Pacific region, the solar signal appears to exclusively and significantly manifest in the APSJ center. We thus aim to give a possible explanation for this interesting phenomenon in this section. To cover the zonal range of the APSJ center (125°E–160°E), the DJF-mean zonal wind and meridional circulation are zonally averaged over 105°E–180°E. Then, we calculate their correlations with the APSJ center intensity index based on the ERA-Interim dataset (Fig. 5). The vertical structure of zonal wind related to the APSJ center intensity exhibits a tripolar banded pattern with positive correlations over the subtropics and negative correlations in the equatorward and poleward sides. Significant meridional circulations present not only in the tropical troposphere but also in the middle–high latitude stratosphere and troposphere. Here, we only consider the top–down transfer of solar signal from the stratosphere to the troposphere. The results shown in Fig. 5 suggest that the solar signal could influence the APSJ via two routes, a tropical route and a middle–high latitude route. In the tropical route, solar activity could affect the APSJ with the aid of regional tropical troposphere circulation (i.e. Hadley cell). In the middle–high latitude route, stratospheric and tropospheric circulations at the middle–high latitudes could avail the downward propagation of solar signal. These two routes of top–down mechanism are analyzed to clarify why solar signal particularly manifests at the APSJ center.

4.1 Tropical route

Due to the fact that the impact of solar activity on the troposphere might not be comparable to that of ENSO in certain areas, some important regional solar signals in the tropical and subtropical troposphere could be masked by ENSO signals. Therefore, in this analysis, the wintertime ENSO signal was removed from the climate variables by performing the linear regression to avoid interference.

Evidence indicated that the variation in the strength of East Asian subtropical jet was closely related to the convection over the maritime continent and tropical western Pacific (Lau and Boyle 1987; Park and An 2014; Guo et al. 2015). Moreover, the tropical convection was yielding to solar modulation according to Labitzke and van Loon (1995) and Xiao et al. (2016). Therefore, we calculate the correlations of OLR (with the wintertime ENSO signal removed) with the APSJ center intensity index (× − 1.0) and SSN in winter (Fig. 6). The weakening of APSJ center westerlies positively associates with OLR in the tropical Western

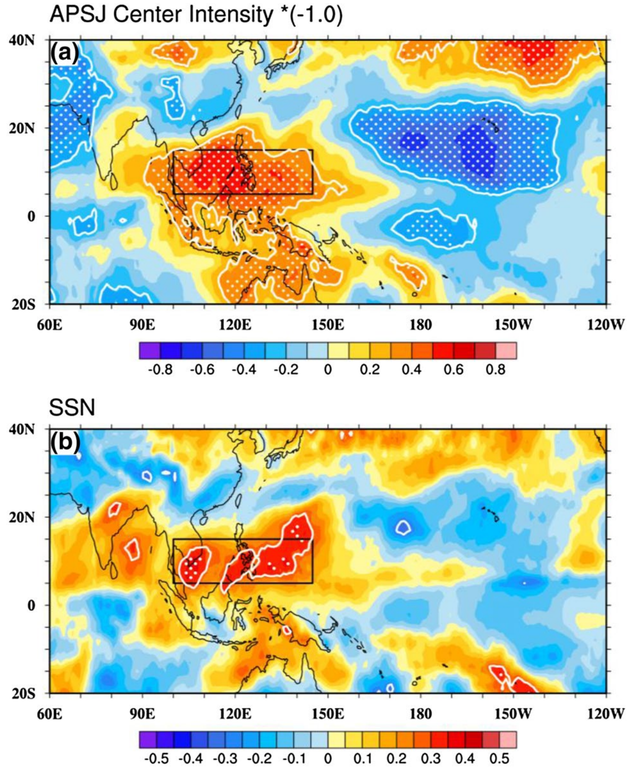

Fig. 6 Correlations of DJF OLR (with the winter ENSO signal removed) with DJF **a** APSJ center intensity index (× − 1.0) and **b** SSN. White dots (white contours) indicate the 95% (90%) confidence level or above. Box (5°N–15°N, 100°E–145°E) represents the main significant areas in both **a** and **b**

Pacific and the maritime continent and negatively correlates with OLR within 160°E–140°W in the tropical North Pacific at the 95% confidence level (Fig. 6a). This means that the weakened APSJ center corresponds to the suppressed local convection over the maritime continent and tropical western Pacific. The OLR that significantly and positively correlated with SSN mainly presents in the tropical Northwest Pacific (see the box in Fig. 6b), hinting that this regional tropical upwelling could be suppressed under increased solar forcing. It is noteworthy that the significant correlations in Fig. 6a, b steadily mark the same area over the South China seas and tropical western Pacific. Therefore, we hypothesize that the close relationship between APSJ center intensity and solar activity could be established via solar impact on the local tropical convection.

To support this hypothesis, we compute the correlations of zonal mean (105°E–180°E) residual meridional circulation, ozone mass mixing ratio, air temperature, and zonal wind with SSN in boreal winter, as exhibited in the latitude-height cross-sections in Fig. 7. Accompanied with the reduced Brewer–Dobson circulation (BDC) in the stratosphere, the ozone density response to the increased solar forcing shows a significant positive correlation in the tropical lower stratosphere (30–50 hPa) (Fig. 7a). Specifically, the solar-associated anomalous subsidence of residual meridional circulation within 15°N–35°N could transport the ozone-rich air from the middle-upper stratosphere to the lower stratosphere. Such increased ozone concentrations could create positive air temperature anomalies at

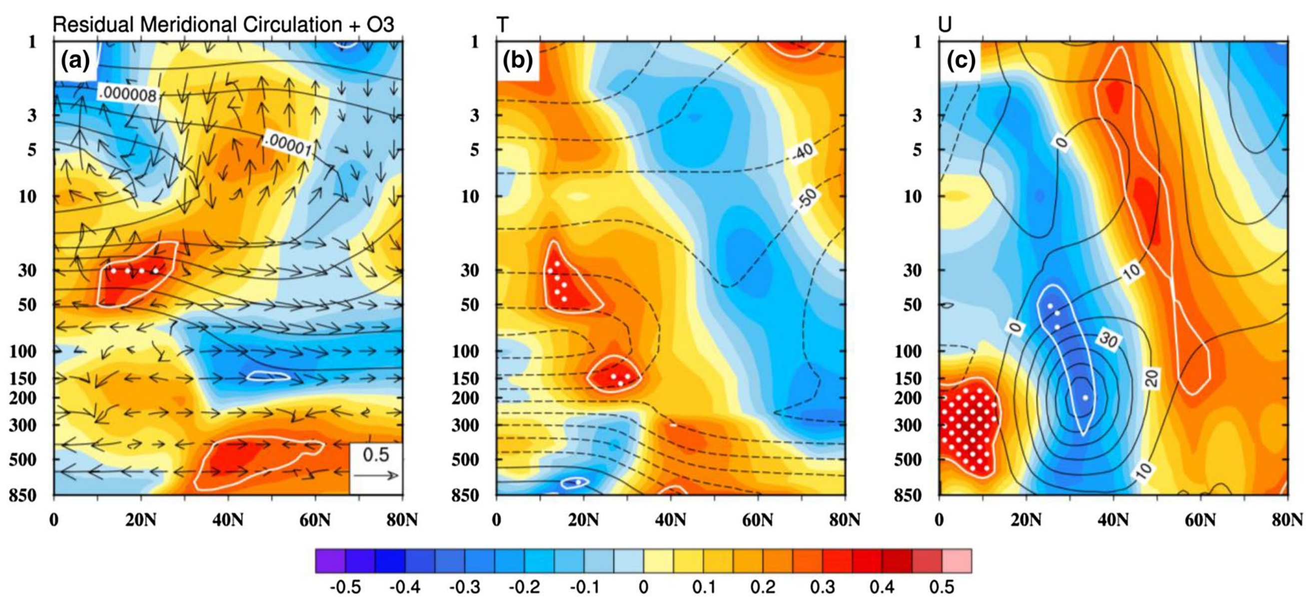

Fig. 7 Correlations of DJF zonal mean (105°E–180°E) **a** residual meridional circulation (arrows) and ozone mass mixing ratio (color shading), **b** air temperature, and **c** zonal wind with DJF SSN. Black contours represent the climatology for the winters of 1980–2015. Contour intervals in **a–c** are 0.00002 kg/kg, 10 °C, and 10 m s^{-1}, respectively. The winter ENSO signal in these climate variables have been removed. Correlations above the 95% (90%) confidence levels are highlighted with white dots (white contours)

95% confidence level in the tropics of lower stratosphere and upper troposphere (Fig. 7b) by ozone heating. Besides, the anomalous downwelling of BDC itself could produce dynamic heating in the tropical lower stratosphere (Matthes et al. 2006). Haigh et al. (2005) and Simpson et al. (2009) hinted that the heating in the tropical lower stratosphere could be a possible origin of solar impact on the troposphere, and the lower stratospheric warming in tropics could suppress the tropical convection and vertical motion of troposphere (Thuburn and Craig 2000; Gleisner and Thejll 2003; Matthes et al. 2006). Hence, the slight subsidence in the tropospheric upwelling around 10°N in Fig. 7a and the weakened OLR over the tropical western North Pacific in Fig. 6b, which are indicative of the reduced rising branch of local Hadley cell, could result from this lower stratospheric warming at tropics in Fig. 7b. The Hadley cell generally acts as 'a transportation' from tropics to subtropics. Along with the weakening in ascending branch of the regional Hadley cell, westerlies in the APSJ center decrease markedly (Fig. 7c). When the wintertime ENSO signal was removed from the zonal wind field, significant decreases in the zonal mean (105°E–180°E) zonal wind due to stronger solar activity still appear in the APSJ center (Fig. 7c), supporting the possibility that the APSJ center's sensitivity to external solar forcing might be independent of the ENSO. The observed vertical structures of stratospheric regional circulation, ozone, air temperature, and zonal wind in response to solar forcing in this analysis are similar to those based on zonally averaged fields in previous studies (e.g. Crooks and Gray 2005; Haigh et al. 2005; Matthes et al. 2006; Hood and Soukharev 2012).

Although the above tropical route of 'top–down' mechanism seems plausible, the preference for the APSJ center as an exclusive region by solar activity remains to be explained. Therefore, the solar association with the meridional mean (10°N–30°N) ozone mass mixing ratio and zonal circulation is inspected based on the longitude–height cross-sections exhibited in Fig. 8. The pronounced positive correlations between SSN and ozone mass mixing ratio with 95% confidence level particularly dominate the lower stratosphere (30–50 hPa) overlying the APSJ center. As indicated by the vectors of zonal circulation related to SSN in Fig. 8, the possible explanation for this notable regional increase in ozone concentrations can fall into two aspects: one is that the tropical anomalous descending motions of BDC in the stratosphere forced by higher solar activity could transport the ozone-rich air to this area; the other is that the slight joining and dispersing of the anomalous winds lying to the east and west of this significant area could assist the regional rise in ozone concentrations.

To clarify this tropical top–down propagation of solar signal in the Asian–Pacific sector, we further examine the longitude-time distributions of correlations of the DJF-mean

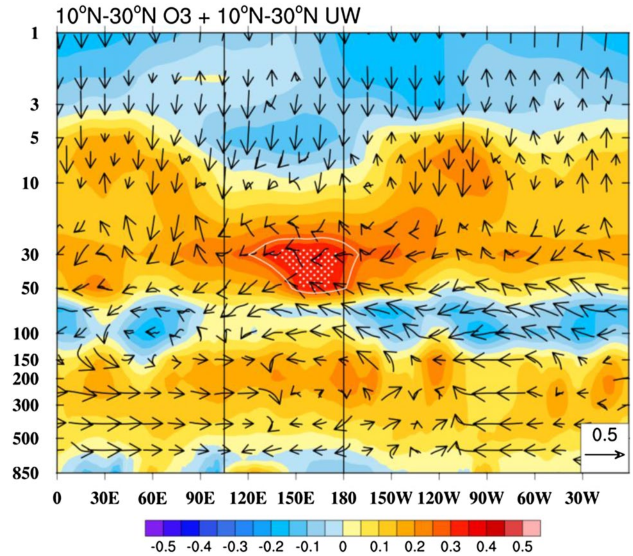

Fig. 8 As in Fig. 7a, but for the meridional mean (10°N–30°N) zonal circulation (arrows) and meridional mean (10°N–30°N) ozone mass mixing ratio (color shading)

SSN with monthly regional zonal mean 30 hPa ozone mass mixing ratio, 50 hPa air temperature, OLR, 300 hPa vertical wind, and 200 hPa zonal wind in extended winter (October to March) (Fig. 9). The marked positive correlations between the tropical 30 hPa ozone concentration and SSN within the zonal range of APSJ center can be first observed in November (Fig. 9a). Then in December, due to ozone heating, significant warming of the air at 50 hPa related to increased SSN begins to occupy the tropical Asian–Pacific (Fig. 9b). With such heating in the tropical lower stratosphere, the significant suppressed regional OLR and 300 hPa upward motion first appear over 100°E–120°E in December (Fig. 9c, d). Then in January, interestingly, these significant regions shift eastward by about 20–25 longitudes (Fig. 9c, d). The pronounced weakened convection and rising motion in January, whose longitudinal positions are quite consistent with the APSJ center, simultaneously cause an obvious deceleration in APSJ center in January (Fig. 9e) with the aid of local Hadley cell. These findings illustrated in the longitude-time evolution of monthly correlations in Fig. 9 further support that the preferred solar signal could transfer from the tropical stratosphere to the subtropical troposphere with time. In summary, during boreal winter, led by the reduction of BDC associated with increased solar forcing, the significant higher ozone concentration in the tropical lower stratosphere only appears within the zonal range of APSJ center, then heating the air here. Thereby, the regional tropical convection in the troposphere is suppressed due to this anomalous warming, consequently resulting in a significant deceleration in APSJ center through the weakened local Hadley cell.

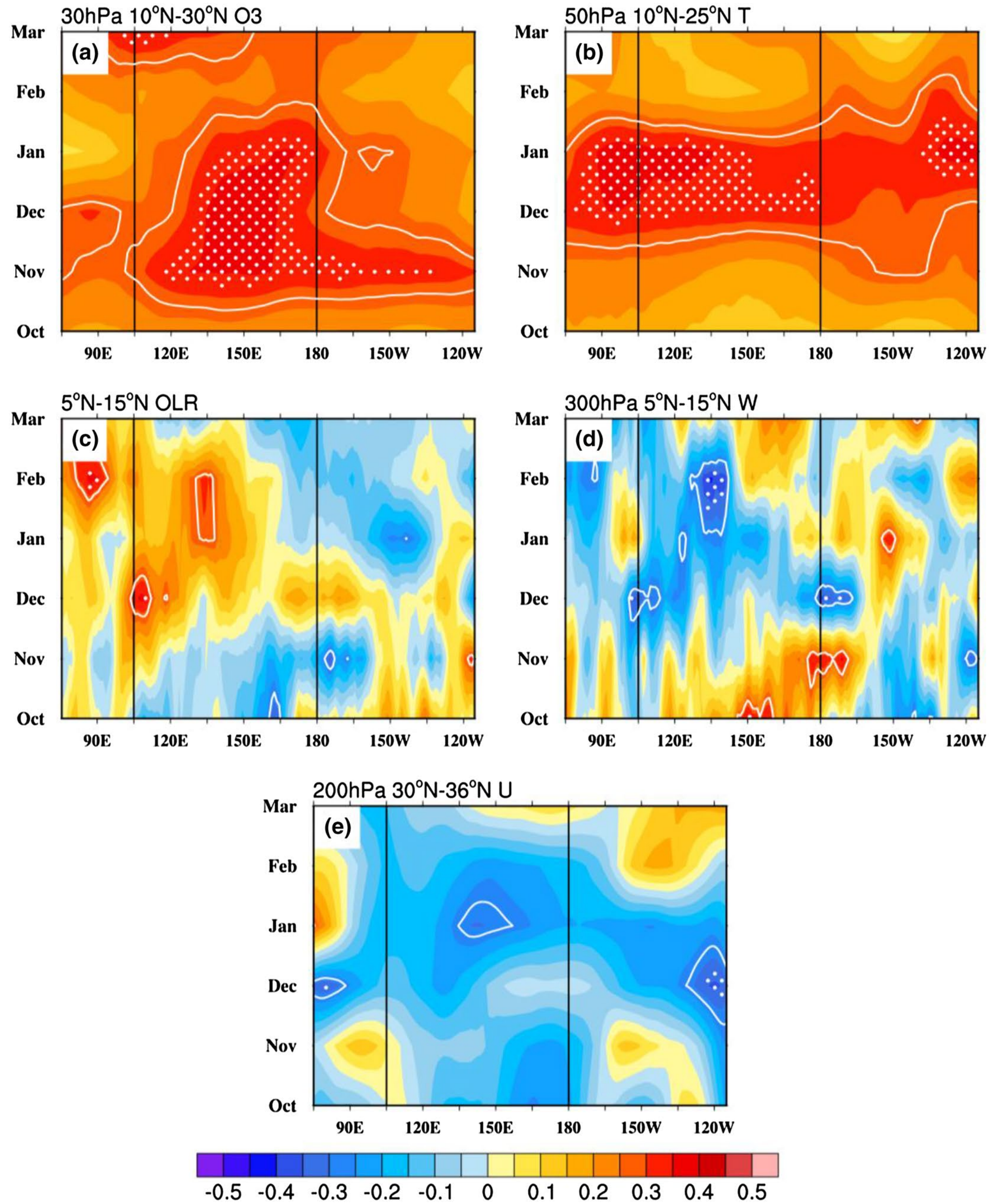

Fig. 9 Longitude-time distributions of the correlations of DJF SSN with monthly meridional mean **a** (10°N–30°N) 30 hPa ozone mass mixing ratio, **b** (10°N–25°N) 50 hPa air temperature, **c** (5°N–15°N) OLR, **d** (5°N–15°N) 300 hPa vertical wind, and **e** (30°N–36°N) 200 hPa zonal wind in extended winter (October–March). The wintertime ENSO signal was removed from all climate variables before performing the calculations. The white dots (white contours) indicate correlations above the 95% (90%) confidence level

4.2 Middle–high latitude route

During the cold season, assisted by the perturbation of stratospheric zonal flow at middle–high latitudes, solar signal could transmit to the troposphere through a top–down stratospheric pathway (e.g. Kodera and Kuroda 2002; Matthes et al. 2006; Ineson et al. 2011; Kodera et al. 2016). To determine how the solar signal propagates downward and equatorward from the stratosphere to the APSJ through a middle–high latitude route, we first give the association between stratospheric zonal wind and SSN (Fig. 10). It is striking that the positive correlations between SSN and zonal wind at 5 hPa with a 90% confidence level merely mark the area of (40°N–50°N, 105°E–145°E) over East Asia (Fig. 10a). Moreover, the pronounced intensified westerlies connected to solar activity only occur at 20–2 hPa in the

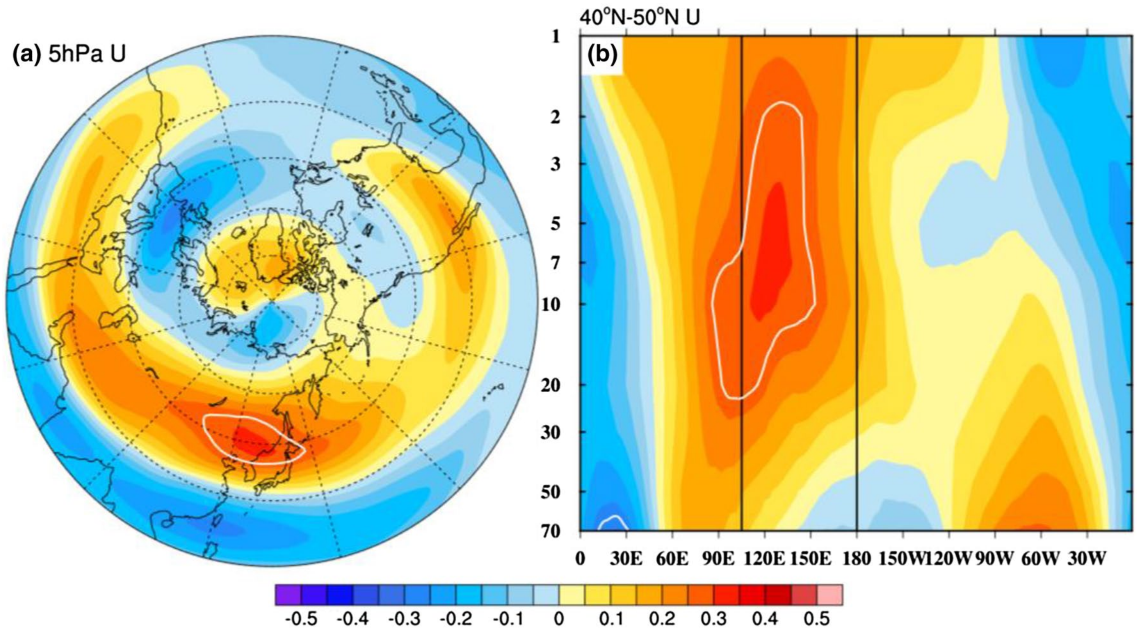

Fig. 10 **a** Correlations between DJF 5 hPa zonal wind and DJF SSN. **b** Correlations between DJF meridional mean (40°N–50°N) zonal wind at 70–1 hPa and DJF SSN. White contours indicate the 90% confidence level or above (no areas reach 95% confidence level in this figure)

longitudinal range of APSJ center (Fig. 10b), reflecting solar preference of this area in the stratospheric zonal wind.

As proposed previously, the enhanced meridional temperature gradient in the stratosphere caused by increased solar shortwave heating produced stronger zonal mean zonal wind in the upper-stratospheric subtropics in early winter, and this accelerated westerly wind affected the planetary waves propagation, as winter progresses, atmospheric circulations in stratosphere and troposphere could be altered via the wave mean flow interactions (Kodera 1995; Kodera and Kuroda 2002; Matthes et al. 2004, 2006; Kodera et al. 2016). Following these studies, based on the ERA-Interim dataset from November 1979 to March 2015, we display the monthly evolution of correlations between DJF-mean SSN and monthly air temperature at 5 hPa within the Asian–Pacific sector, zonal mean (105°E–180°E) zonal wind, Eliassen–Palm (E–P) flux (indicating the direction of planetary wave propagation) and its divergence (a measure of wave mean flow interactions) from November to March (Fig. 11). In early winter, due to increased solar forcing, the meridional temperature gradient at 5 hPa between the low and high latitudes of the Asian–Pacific region grows from November to December, leading to a significant acceleration in stratospheric zonal wind at mid-latitudes of 40°N–50°N. The upward propagating planetary waves from the troposphere could be reflected back downward by the anomalous westerlies in the subtropical stratosphere (Kodera and Kuroda 2002; Matthes et al. 2006; Kodera et al. 2016), and the anomalous E–P flux moves downward and poleward in the middle–high latitude stratosphere and upper-troposphere in November and December. As a result of positive feedback between planetary wave and zonal mean flow, the significant strengthened westerlies in the stratosphere shift to higher latitudes (~60°N) of the troposphere in January. Meanwhile, in January the tropospheric E–P flux anomalies turn to propagate equatorward. With this enhanced equatorward propagating planetary waves in the troposphere, the notable anomalous convergence of E–P flux at 20°N–40°N near the tropopause consequently decelerates the upper-tropospheric zonal wind around the APSJ center in January. Hence, a significant weakened tropospheric SJ can be seen in January. Then in February, the tropospheric planetary waves continue to move equatorward, and the pronounced weakened westerlies in subtropics can be found near the tropopause. No significant correlations between SSN and zonal mean (105°E–180°E) zonal wind are observed in March. In summary, as winter progresses, the solar signal can transfer from the middle–high latitude stratosphere to the subtropical troposphere through wave mean flow interactions, resulting in a significant weakened APSJ center in the middle of winter. Note that, in early winter, the accelerated westerlies in the mid-latitude stratosphere created by solar forcing particularly emerge within the zonal range of APSJ center, further confirming that the APSJ center could be an exclusive region for the spread of solar signal.

We should point out that the two top–down routes discussed in Sects. 4.1 and 4.2 cannot be completely separated. In early winter, the deflection of planetary waves associated

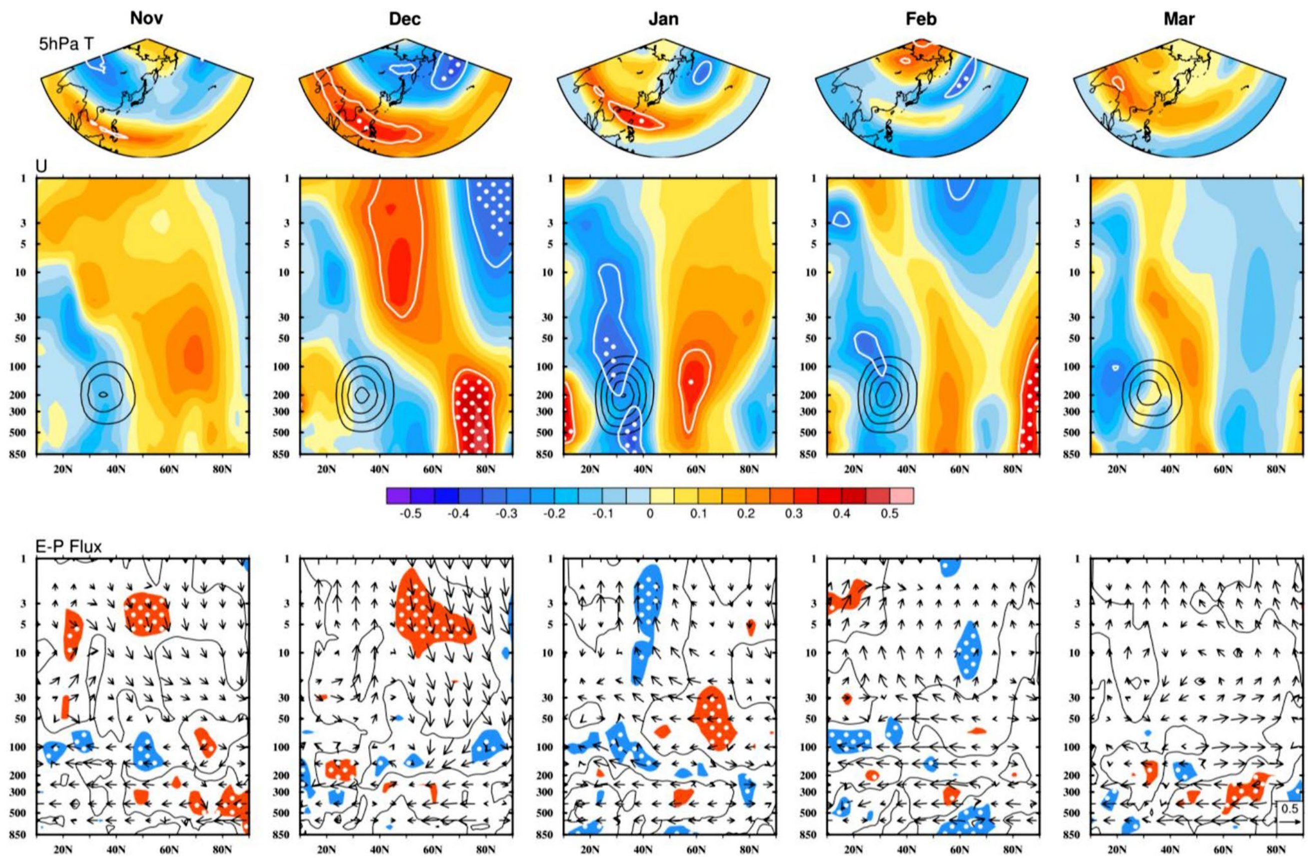

Fig. 11 Correlations between DJF SSN and monthly (top) air temperature at 5 hPa, (middle) zonal mean (105°E–180°E) zonal wind, and (bottom) E–P flux (vectors) and its divergence (contours) from November to March. Areas above the 95% (90%) significance are highlighted by white dots (white contours) in the top and middle panels. In the middle panel, the average zonal mean (105°E–180°E) zonal wind speed exceeding 30 m s^{-1} is represented by black contours in intervals of 10 m s^{-1}. Black contours in the bottom panel indicate the zero lines of the correlations between E–P flux divergence and SSN, and only positive (negative) correlations above the 90% confidence level are shaded in orange (blue). White dots in the bottom panel indicate the 95% confidence level or above

with solar-induced stratospheric perturbation could also cause the weakening of BDC (Kodera and Kuroda 2002). Although similar mechanisms of solar influence on tropospheric circulation have been revealed previously, the present study offers a possible explanation of why the solar signal manifests only in the APSJ center. Surprisingly, the significant increased ozone concentration of the tropical lower stratosphere and accelerated westerlies of the midlatitude stratosphere, which are closely tied to intensified solar forcing, exclusively appear within the zonal range of APSJ center (Figs. 8, 10). These key findings provide strong evidence to support solar preference of the APSJ center.

5 Conclusion and discussion

Unlike some previous studies that investigated solar influence on the tropospheric SJ from a zonally averaged perspective, we focus on revealing the particular solar signal and its transfer in the regional SJ within the Asian–Pacific sector. Based predominantly on observational data over the last three solar cycles, we found some intriguing results. In boreal winter, the second internal mode for the variability of 200 hPa zonal wind over the Asian–Pacific region, which shows a banded structure with easterly anomalies over the subtropics and westerly anomalies on the poleward and equatorward sides, bears great resemblance to the solar-induced tripolar pattern of 200 hPa zonal wind in the same sector. Strikingly, significant response of the APSJ to higher solar activity only marks its center, appearing as a deceleration in westerlies. Following several studies on the top–down transfer of solar signal (e.g. Kodera and Kuroda 2002; Matthes et al. 2006; Kodera et al. 2016), we suggest two plausible top–down routes to interpret the preference of the solar signal for the tropospheric APSJ center, a tropical route (Fig. 12a) and a middle–high latitude route (Fig. 12b). For the tropical route, during the cold season, driven by the reduced stratospheric BDC in response to increased solar forcing, the significant higher ozone concentration presents in the tropical lower stratosphere, then heating the air here.

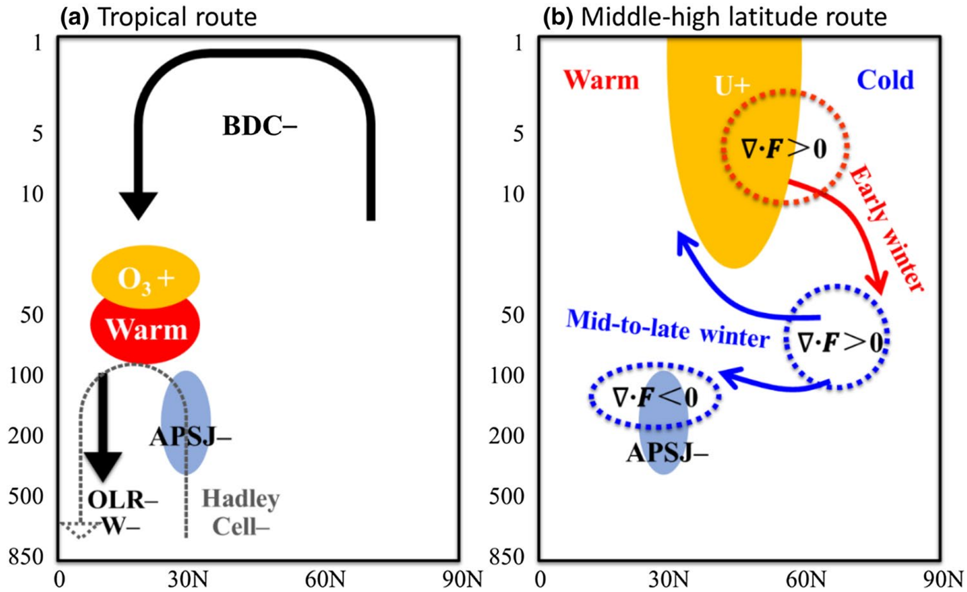

Fig. 12 Schematic illustration of **a** the tropical route and **b** the middle–high latitude route for the top–down transfer of solar signal from the stratosphere to the tropospheric APSJ center during boreal winter. The two routes are related, although two separate diagrams are shown here. The processes in **a** sequentially contain the anomalous reduced BDC (black arrow in the stratosphere), increased ozone concentration (yellow filled contour), warm air (red filled contour), suppressed vertical movement or OLR (black arrow in the troposphere), weakened Hadley cell (dashed grey arrows), and decelerated westerlies in the APSJ center (blue filled contour). The processes in **b** are divided into two periods, early winter (red arrows and circles) and mid-to-late winter (blue arrows and circles). The yellow and blue filled contours in **b** respectively indicate the strengthened westerlies in mid-latitude stratosphere and the weakened APSJ center. $\nabla \cdot \boldsymbol{F} > 0$ (<0) represents the anomalous divergence (convergence) of E–P flux. The anomalous propagation of planetary waves is indicated by arrows. See Sects. 4 and 5 for more details

The regional convection (rising motion) in the tropical troposphere is thereby suppressed. Consequently, a marked deceleration in the APSJ center is produced via the weakened local Hadley cell. For the middle–high latitude route, winter can be divided into two periods, the early winter dominated by solar radiative forcing and the late winter dominated by tropospheric dynamical forcing (Kodera and Kuroda 2002; Kodera et al. 2016). In early winter, due to the anomalous low-latitude warming and high-latitude cooling associated with increased solar radiative forcing, anomalous westerlies emerge in the mid-latitude stratosphere. The planetary waves can be deflected by this anomalous westerly wind in stratosphere. Then, in mid-to-late winter, the anomalous enhanced planetary waves in troposphere propagate equatorward. Through the wave mean flow interactions, a resultant significant weakened APSJ center can be observed in the middle of winter. There is an association between the strengthening of mid-latitude stratospheric zonal wind and the deceleration of BDC (Kodera and Kuroda 2002). Therefore, these two possible top–down routes should not be separated entirely, and their combination results in the downward extension of solar signal over the Asian–Pacific sector. Note that, both the area of significant increased ozone concentration in the tropical lower stratosphere in Fig. 8 and the region with pronounced strengthened westerlies in the mid-latitude stratosphere in Fig. 10 correspond well to the zonal location of the APSJ center. Both make the APSJ center appear as a region particularly preferred by solar signal. Therefore, our findings do have implications for the question of where the sun exerts its influence on the troposphere. Because of the lack in quantitative analyses for the possible mechanisms presented in this paper, it is necessary to probe into the accurate processes with the help of numerical models in further.

Ruzmaikin (1999) pointed out that, as a stochastic driver, ENSO can make the 11-year solar cycle forcing of climate feasible. However, for revealing the top–down transfer of solar signal over the Asian–Pacific sector more clearly, we simply removed the ENSO signal in climate variables in Sect. 4.1, making it harder to find the bottom-up mechanism of solar signal transfer. The idealized numerical experiments conducted by Nakamura et al. (2008) demonstrated the importance of mid-latitude oceanic frontal zones, characterized by the sharp meridional gradient of SST, for the tropospheric circulation and its variability. Therefore, the SJ over the Asian–Pacific region could be influenced by the strong mid-latitude oceanic frontal zone off the east coast of Asia, to a degree. However, the potential effects of oceanic fronts have not been considered in the present study. In addition, Zhou et al. (2013) indicated that the effect of ENSO on the wintertime regional climate over Asia and North Pacific was strongly modulated by solar cycle. It hints that the solar impacts on the Asian–Pacific regional climate might be indirect and some important air–sea coupled systems could act as media to transfer the solar signal to the Asian–Pacific region. Therefore, subsequent studies should pay attention to the role of air–sea interaction in modulating the regional solar signal in the Asian–Pacific sector. Besides, in response to positive AO, the robust lower tropospheric warming in northeastern Asia can be found during high solar activity winters, which appeared to result from the solar-related active coupling between stratosphere and troposphere (Chen and Zhou 2012). Moreover, the close association between AO and tropospheric subtropical jet stream is well known (e.g. Ambaum et al. 2001; Gong and Ho 2003; Hinssen et al. 2010). But we have not taken into account the response of AO to solar forcing in the middle–high latitude route for solar signal downward transfer in the APSJ. So, this needs to be discussed in further study.

Acknowledgements The authors appreciate the helpful suggestions from Dr. Katja Matthes. This work was jointly supported by the National Natural Science Foundation of China (91637208), the National Basic Research Program of China (2012CB957804), the Natural Science Foundation of China (41305131), and the Key Project of Natural Science Foundation of Yunnan (2016FA041).

References

Ambaum MHP, Hoskins BJ, Stephenson DB (2001) Arctic oscillation or North Atlantic oscillation? J Clim 14(16):3495–3507. https://doi.org/10.1175/1520-0442(2001)014%3C3495:AOONAO%3E2.0.CO;2

Andreoli RV, Kayano MT (2005) ENSO-related rainfall anomalies in South America and associated circulation features during warm and cold Pacific decadal oscillation regimes. Int J Climatol 25:2017–2030. https://doi.org/10.1002/joc.1222

Arkin PA (1982) The relationship between interannual variability in the 200 mb tropical wind field and the Southern Oscillation. Mon Weather Rev 110:1393–1404. https://doi.org/10.1175/1520-0493(1982)110%3C1393:TRBIVI%3E2.0.CO;2

Baldwin MP, Dunkerton TJ (1999) Propagation of the Arctic Oscillation from the stratosphere to the troposphere. J Geophys Res 104(D24):30937–30946. https://doi.org/10.1029/1999JD900445

Chen WY, van den Dool HM (1999) Significant change of extratropical natural variability and potential predictability associated with the El Nino/Southern Oscillation. Tellus 51A:790–802. https://doi.org/10.1034/j.1600-0870.1999.00017.x

Chen W, Zhou Q (2012) Modulation of the Arctic Oscillation and the East Asian winter climate relationships by the 11-year solar cycle. Adv Atmos Sci 29:217–226. https://doi.org/10.1007/s00376-011-1095-3

Codron F (2007) Relations between annular modes and the mean state: Southern Hemisphere winter. J Atmos Sci 64:3328–3339. https://doi.org/10.1175/JAS4012.1

Crooks SA, Gray LJ (2005) Characterization of the 11-year solar signal using a multiple regression analysis of the ERA-40 dataset. J Clim 18:996–1015. https://doi.org/10.1175/JCLI-3308.1

Dee DP, Uppala SM, Simmons AJ, Berrisford P, Poli P, Kobayashi S, Andrae U, Balmaseda MA, Balsamo G, Bauer P, Bechtold P, Beljaars ACM, van de Berg L, Bidlot J, Bormann N, Delsol C, Dragani R, Fuentes M, Geer AJ, Haimberger L, Healy SB, Hersbach H, Hólm EV, Isaksen L, Kållberg P, Köhler M, Matricardi M, McNally AP, Monge-Sanz BM, Morcrette JJ, Park BK, Peubey C, de Rosnay P, Tavolato C, Thépaut JN, Vitart F (2011) The ERA-Interim reanalysis: configuration and performance of the data assimilation system. Q J R Meteorol Soc 137(656):553–597. https://doi.org/10.1002/qj.828

Gleisner H, Thejll P (2003) Patterns of tropospheric response to solar variability. Geophys Res Lett 30:1711. https://doi.org/10.1029/2003GL017129

Gong DY, Ho CH (2003) Arctic oscillation signals in the East Asian summer monsoon. J Geophys Res 108:4066. https://doi.org/10.1029/2002JD002193

Gray LJ, Scaife AA, Mitchell DM, Osprey S, Ineson S, Hardiman S, Butchart N, Knight J, Sutton R, Kodera K (2013) A lagged response to the 11 year solar cycle in observed winter Atlantic/European weather patterns. J Geophys Res Atmos 118:13405–13420. https://doi.org/10.1002/2013JD020062

Guo Y, Wen Z, Wu R, Lu R, Chen Z (2015) Impact of tropical Pacific precipitation anomaly on the East Asian upper-tropospheric westerly jet during the boreal winter. J Clim 28:6457–6474. https://doi.org/10.1175/JCLI-D-14-00674.1

Haigh JD (1996) The impact of solar variability on climate. Science 272:981–984. https://doi.org/10.1126/science.272.5264.981

Haigh JD, Blackburn M (2006) Solar influences on dynamical coupling between the stratosphere and troposphere. Space Sci Rev 125:331–344. https://doi.org/10.1007/s11214-006-9067-0

Haigh JD, Blackburn M, Day R (2005) The response of tropospheric circulation to perturbations in lower stratospheric temperature. J Clim 18:3672–3691. https://doi.org/10.1175/JCLI3472.1

Hinssen Y, van Delden A, Opsteegh T, de Geus W (2010) Stratospheric impact on tropospheric winds deduced from potential vorticity inversion in relation to the Arctic Oscillation. Q J R Meteorol Soc 136:20–29. https://doi.org/10.1002/qj.542

Hong X, Lu R (2016) The meridional displacement of the summer Asian jet, Silk Road pattern, and tropical SST anomalies. J Clim 29:3753–3766. https://doi.org/10.1175/JCLI-D-15-0541.1

Hood LL, Soukharev BE (2012) The lower stratospheric response to 11-yr solar forcing: coupling to the troposphere–ocean response. J Atmos Sci 69:1841–1863. https://doi.org/10.1175/JAS-D-11-086.1

Huth R, Pokorná L, Bochníček J, Hejda P (2006) Solar cycle effects on modes of low-frequency circulation variability. J Geophys Res 111:D22107. https://doi.org/10.1029/2005JD006813

Ineson S, Scaife AA, Knight JR, Manners JC, Dunstone NJ, Gray LJ, Haigh JD (2011) Solar forcing of winter climate variability in the Northern Hemisphere. Nat Geosci 4:753–757. https://doi.org/10.1038/ngeo1282

Jhun JG, Lee EJ (2004) A new East Asian winter monsoon index and associated characteristics of the winter monsoon. J Clim 17:711–726. https://doi.org/10.1175/1520-0442(2004)017%3C0711:ANEAWM%3E2.0.CO;2

Kalnay E, Kanamitsu M, Kistler R, Collins W, Deaven D, Gandin L, Iredell M, Saha S, White G, Woollen J, Zhu Y, Leetmaa A, Reynolds R, Chelliah M, Ebisuzaki W, Higgins W, Janowiak J, Mo KC, Ropelewski C, Wang J, Jenne R, Joseph D (1996) The NCEP/NCAR 40-year reanalysis project. Bull Am Meteorol Soc 77(3):437–471. https://doi.org/10.1175/1520-0477(1996)077%3C0437:TNYRP%3E2.0.CO;2

Kodera K (1995) On the origin and nature of the interannual variability of the winter stratospheric circulation in the Northern Hemisphere. J Geophys Res 100:14077–14087. https://doi.org/10.1029/95JD01172

Kodera K (2002) Solar cycle modulation of the North Atlantic Oscillation: implication in the spatial structure of the NAO. Geophys Res Lett 29:1218. https://doi.org/10.1029/2001GL014557
Kodera K (2003) Solar influence on the spatial structure of the NAO during the winter 1900–1999. Geophys Res Lett 30:1175. https://doi.org/10.1029/2002GL016584
Kodera K, Kuroda Y (2002) Dynamical response to the solar cycle. J Geophys Res 107:4749. https://doi.org/10.1029/2002JD002224
Kodera K, Kuroda Y (2005) A possible mechanism of solar modulation of the spatial structure of the North Atlantic Oscillation. J Geophys Res 110:D02111. https://doi.org/10.1029/2004JD005258
Kodera K, Thiéblemont R, Yukimoto S, Matthes K (2016) How can we understand the global distribution of the solar cycle signal on the Earth's surface? Atmos Chem Phys 16:12925–12944. https://doi.org/10.5194/acp-16-12925-2016
Kuang X, Zhang Y (2005) Seasonal variation of the East Asian subtropical westerly jet and its association with the heating field over East Asia. Adv Atmos Sci 22:831–840. https://doi.org/10.1007/BF02918683
Kuroda Y, Kodera K (2005) Solar cycle modulation of the Southern Annular Mode. Geophys Res Lett 32:L13802. https://doi.org/10.1029/2005GL022516
Kuroda Y, Shibata K (2006) Simulation of solar-cycle modulation of the Southern Annular Mode using a chemistry-climate model. Geophys Res Lett 33:L05703. https://doi.org/10.1029/2005GL025095
Kuroda Y, Yamazaki K (2010) Influence of the solar cycle and QBO modulation on the Southern Annular Mode. Geophys Res Lett 37:L12703. https://doi.org/10.1029/2010GL043252
Kushner PJ, Polvani LM (2004) Stratosphere–troposphere coupling in a relatively simple AGCM: the role of eddies. J Clim 17:629–639. https://doi.org/10.1175/1520-0442(2004)017%3C0629:SCIARS%3E2.0.CO;2
Labitzke K, van Loon H (1995) Connection between the troposphere and stratosphere on a decadal scale. Tellus 47A:275–286. https://doi.org/10.1034/j.1600-0870.1995.t01-1-00008.x
Lau KM, Boyle JS (1987) Tropical and extratropical forcing of the large-scale circulation—a diagnostic study. Mon Weather Rev 115:400–428. https://doi.org/10.1175/1520-0493(1987)115%3C0400:TAEFOT%3E2.0.CO;2
Lee HT (2014) Climate algorithm theoretical basis document (C-ATBD): outgoing longwave radiation (OLR)—daily. NOAA's climate data record (CDR) program. CDRP-ATBD-0526, p 46
Li J, Wang JXL (2003) A modified zonal index and its physical sense. Geophys Res Lett 30:1632. https://doi.org/10.1029/2003GL017441
Li D, Xiao Z (2018) Can solar cycle modulate the ENSO effect on the Pacific/North American pattern? J Atmos Sol Terr Phys 167:30–38. https://doi.org/10.1016/j.jastp.2017.10.007
Liang X, Wang W (1998) Associations between China monsoon rainfall and tropospheric jets. Q J R Meteorol Soc 124:2961–3012. https://doi.org/10.1002/qj.49712455204
Limpasuvan V, Hartmann DL (2000) Wave-maintained annular modes of climate variability. J Clim 13:4414–4429. https://doi.org/10.1175/1520-0442(2000)013,4414:WMAMOC.2.0.CO;2
Lin Z, Lu R (2005) Interannual meridional displacement of the East Asian upper-tropospheric jet stream in summer. Adv Atmos Sci 22:300–312. https://doi.org/10.1007/BF02918519
Liu Z, Yoshimura K, Buenning NH, He X (2014) Solar cycle modulation of the Pacific–North American teleconnection influence on North American winter climate. Environ Res Lett 9:024004. https://doi.org/10.1088/1748-9326/9/2/024004
Matthes K, Langematz U, Gray LL, Kodera K, Labitzke K (2004) Improved 11-year solar signal in the Freie Universität Berlin Climate Middle Atmosphere Model (FUB-CMAM). J Geophys Res 109:D06101. https://doi.org/10.1029/2003JD004012
Matthes K, Kuroda Y, Kodera K, Langematz U (2006) Transfer of the solar signal from the stratosphere to the troposphere: Northern winter. J Geophys Res 111:D06108. https://doi.org/10.1029/2005JD006283
Meehl GA, Arblaster JM, Matthes K, Sassi F, van Loon H (2009) Amplifying the Pacific climate system response to a small 11-year solar cycle forcing. Science 325:1114–1118. https://doi.org/10.1126/science.1172872
Misios S, Schmidt H (2013) The role of the oceans in shaping the tropospheric response to the 11 year solar cycle. Geophys Res Lett 40:6373–6377. https://doi.org/10.1002/2013GL058439
Nakamura H, Sampe T, Goto A, Ohfuchi W, Xie SP (2008) On the importance of midlatitude oceanic frontal zones for the mean state and dominant variability in the tropospheric circulation. Geophys Res Lett 35:L15709. https://doi.org/10.1029/2008GL034010
Oort AH, Yienger JJ (1996) Observed interannual variability in the Hadley circulation and its connection to ENSO. J Clim 9:2751–2767. https://doi.org/10.1175/1520-0442(1996)009%3C2751:OIVITH%3E2.0.CO;2
Park JH, An SI (2014) The impact of tropical western Pacific convection on the North Pacific atmospheric circulation during the boreal winter. Clim Dyn 43:2227–2238. https://doi.org/10.1007/s00382-013-2047-7
Poli P, Hersbach H, Tan D, Dee D, Thépaut J-N, Simmons A, Peubey C, Laloyaux P, Komori T, Berrisford P, Dragani R, Trémolet Y, Holm E, Bonavita M, Isaksen L, Fisher M (2013) The data assimilation system and initial performance evaluation of the ECMWF pilot reanalysis of the 20th-century assimilating surface observations only (ERA-20C). ERA report series 14, ECMWF, p 59
Quadrelli R, Wallace JM (2002) Dependence of the structure of the Northern Hemisphere annular mode on the polarity of ENSO. Geophys Res Lett 29:2132. https://doi.org/10.1029/2002GL015807
Ren X, Zhang Y, Xiang Y (2008) Connections between wintertime jet stream variability, oceanic surface heating, and transient eddy activity in the North Pacific. J Geophys Res 113:D21119. https://doi.org/10.1029/2007JD009464
Rind D, Lean J, Lerner J, Lonergan P, Leboissitier A (2008) Exploring the stratospheric/tropospheric response to solar forcing. J Geophys Res 113:D24103. https://doi.org/10.1029/2008JD010114
Roscoe HK, Haigh JD (2007) Influences of ozone depletion, the solar cycle and the QBO on the Southern Annular Mode. Q J R Meteorol Soc 133:1855–1864. https://doi.org/10.1002/qj.153
Ruzmaikin A (1999) Can El Niño amplify the solar forcing of climate? Geophys Res Lett 26:2255–2259. https://doi.org/10.1029/1999GL900535
Scaife AA, Ineson S, Knight JR, Gray L, Kodera K, Smith DM (2013) A mechanism for lagged North Atlantic climate response to solar variability. Geophys Res Lett 40:434–439. https://doi.org/10.1002/grl.50099
Seager R, Harnik N, Kushnir Y, Robinson WA, Miller JA (2003) Mechanisms of hemispherically symmetric climate variability. J Clim 16(18):2960–2978. https://doi.org/10.1175/1520-0442(2003)016%3C2960:MOHSCV%3E2.0.CO;2
Seager R, Harnik N, Robinson WA, Kushnir Y, Ting M, Huang HP, Velez J (2005) Mechanisms of ENSO-forcing of hemispherically symmetric precipitation variability. Q J R Meteorol Soc 131:1501–1527. https://doi.org/10.1256/qj.04.96
Shindell DT, Rind D, Balachandran N, Lean J, Lonergan P (1999) Solar cycle variability, ozone, and climate. Science 284:305–308. https://doi.org/10.1126/science.284.5412.305
Simpson IR, Blackburn M, Haigh JD (2009) The role of eddies in driving the tropospheric response to stratospheric heating perturbations. J Atmos Sci 66:1347–1365. https://doi.org/10.1175/2008JAS2758.1

Thuburn J, Craig GC (2000) Stratospheric influence on tropopause height: the radiative constraint. J Atmos Sci 57:17–28. https://doi.org/10.1175/1520-0469(2000)057%3C0017:SIOTHT%3E2.0.CO;2
van Loon H, Meehl GA, Arblaster JM (2004) A decadal solar effect in the tropics in July–August. J Atmos Sol Terr Phys 66:1767–1778. https://doi.org/10.1016/j.jastp.2004.06.003
van Loon H, Meehl G, Shea D (2007) Coupled air–sea response to solar forcing in the Pacific region during northern winter. J Geophys Res 112:D02108. https://doi.org/10.1029/2006JD007378
Weng H (2012) Impacts of multi-scale solar activity on climate. Part I: atmospheric circulation patterns and climate extremes. Adv Atmos Sci 29:867–886. https://doi.org/10.1007/s00376-012-1238-1
Xiao Z, Liao Y, Li C (2016) Possible impact of solar activity on the convection dipole over the tropical pacific ocean. J Atmos Sol Terr Phys 140:94–107. https://doi.org/10.1016/j.jastp.2016.02.008
Xie Z, Du Y, Yang S (2015) Zonal extension and retraction of the subtropical westerly jet stream and evolution of precipitation over East Asia and the western Pacific. J Clim 28:6783–6798. https://doi.org/10.1175/JCLI-D-14-00649.1
Yang S, Lau KM, Kim KM (2002) Variations of the East Asian jet stream and Asian–Pacific–American winter climate anomalies. J Clim 15:306–325. https://doi.org/10.1175/1520-0442(2002)015%3C0306:VOTEAJ%3E2.0.CO;2
Zhou Q, Chen W, Zhou W (2013) Solar cycle modulation of the ENSO impact on the winter climate of East Asia. J Geophys Res Atmos 118:5111–5119. https://doi.org/10.1002/jgrd.50453